Corrected 31 October 2022. See full text.



CELL AND GENE THERAPY

# CAR T cells produced in vivo to treat cardiac injury

Joel G. Rurik[1,2,3], István Tombácz[4]†, Amir Yadegari[4]†, Pedro O. Méndez Fernández[1,2,3], Swapnil V. Shewale[2], Li Li[1,2], Toru Kimura[4]‡, Ousamah Younoss Soliman[4], Tyler E. Papp[4], Ying K. Tam[5], Barbara L. Mui[5], Steven M. Albelda[4,6], Ellen Puré[7], Carl H. June[6], Haig Aghajanian[1,2,3]*, Drew Weissman[4]*, Hamideh Parhiz[4]*, Jonathan A. Epstein[1,2,3,4]*

**Fibrosis affects millions of people with cardiac disease. We developed a therapeutic approach to generate transient antifibrotic chimeric antigen receptor (CAR) T cells in vivo by delivering modified messenger RNA (mRNA) in T cell–targeted lipid nanoparticles (LNPs). The efficacy of these in vivo–reprogrammed CAR T cells was evaluated by injecting CD5-targeted LNPs into a mouse model of heart failure. Efficient delivery of modified mRNA encoding the CAR to T lymphocytes was observed, which produced transient, effective CAR T cells in vivo. Antifibrotic CAR T cells exhibited trogocytosis and retained the target antigen as they accumulated in the spleen. Treatment with modified mRNA-targeted LNPs reduced fibrosis and restored cardiac function after injury. In vivo generation of CAR T cells may hold promise as a therapeutic platform to treat various diseases.**

Cardiac fibroblasts become activated in response to various myocardial injuries through well-studied mechanisms including transforming growth factor β–SMAD2/3, interleukin-11, and other interactions with the immune system (*1*–*6*). In many chronic heart diseases, these fibroblasts fail to quiesce and secrete excessive extracellular matrix, resulting in fibrosis (*7*). Fibrosis both stiffens the myocardium and negatively affects cardiomyocyte health and function (*8*). Despite in-depth understanding of activated cardiac fibroblasts, clinical trials of antifibrotic therapeutics have only demonstrated a modest effect (*5*, *7*) at best. Furthermore, these interventions aim to limit fibrotic progression and are not designed to remodel fibrosis once it is established. To address this substantial clinical problem, we recently demonstrated the use of chimeric antigen receptor (CAR) T cells to specifically eliminate activated fibroblasts as a therapy for heart failure (*9*). Elimination of activated fibroblasts in a mouse model of heart disease resulted in a significant reduction of cardiac fibrosis and improved cardiac function (*9*). One caveat of that work is the indefinite persistence of engineered T cells similar to CAR T cell therapy currently used in the oncology clinical setting (*10*). Fibroblast activation is part of a normal wound-healing process in many tissues, and persistent antifibrotic CAR T cells could pose a risk in the setting of future injuries. Therefore, we leveraged the power of nucleoside-modified mRNA technology to develop a transient antifibrotic CAR T therapeutic.

Therapeutic mRNAs can be stabilized by the incorporation of modified nucleosides, synthetic capping, and the addition of lengthy poly-A tails, and can be enhanced with codon optimization (*11*–*13*). 1-Methylpseudouridine integration also boosts translation (*13*, *14*). Direct introduction of mRNA into T cells ex vivo by electroporation has been used successfully by our group and others to make CAR T cells (*15*); however, this process carries significant cost and risk and requires extensive infrastructure. Thus, we developed an approach that could be used to avoid removing T cells from the patient by packaging modified mRNAs in lipid nanoparticles (LNPs) capable of producing CAR T cells in vivo after injection. LNP-mRNA technology underlies recent successes in COVID-19 vaccine development and holds exceptional promise for additional therapeutic strategies (*16*–*20*). Once in the body, mRNA-loaded LNPs, absent of any specific targeting strategies, are endocytosed by various cell types (especially hepatocytes if injected intravenously) (*21*, *22*). Shortly after cellular uptake, the mRNA escapes the endosome, releasing the mRNA into the cytoplasm, where it is transiently transcribed before degrading (*11*). Targeting antibodies can be decorated on the surface of LNPs to direct uptake (and mRNA expression) to specific cell types (*23*, *24*). We hypothesized that an LNP directed to T lymphocytes could deliver sufficient mRNAs to produce functional CAR T cells in vivo (Fig. 1A). Because mRNA is restricted to the cytoplasm and is incapable of genomic integration, intrinsically unstable, and diluted during cell division, these CAR T cells will be, by design, transient.

We generated modified nucleoside-containing mRNA encoding a CAR designed against fibroblast activation protein (FAP) (a marker of activated fibroblasts) and packaged it in CD5-targeted LNPs (referred to as "targeting antibody/LNP-mRNA cargo" or CD5/LNP-FAPCAR) (Fig. 1A) (*9*, *25*). CD5 is naturally expressed by T cells and a small subset of B cells and is not required for T cell effector function (*26*, *27*). As a first proof-of-concept experiment, we incubated CD5/LNPs containing modified mRNA encoding either FAPCAR or green fluorescent protein (GFP) with freshly isolated, activated murine T cells in vitro for 48 hours. CD5-targeted LNPs delivered their mRNA cargo to most T cells in culture, where 81% expressed GFP after exposure to CD5/LNP-GFP (Fig. 1B) and 83% expressed FAPCAR after exposure to CD5/LNP-FAPCAR (Fig. 1, C and D), as measured by flow cytometry (fig. S1A). In vitro, CAR expression peaks at 24 hours and rapidly abates over the ensuing days (fig. S1B). LNPs decorated with isotype control [immunoglobulin G (IgG)] antibodies, and thus not explicitly directed to lymphocytes, were only able to deliver mRNA to a small fraction (7%) of T cells in vitro (Fig. 1, C and D). These LNP-generated CAR T cells were able to effectively kill FAP-expressing target cells in vitro (Fig. 1E) in a dose-dependent manner (fig. S1C) similar to virally engineered FAPCAR T cells. Gene transfer through targeted LNPs in vitro is also possible and efficient (89 to 93%) in human T cells, as demonstrated by targeting ACH2 cells with CD5/LNP-GFP (fig. S1D).

We next assessed whether CD5-targeted LNP mRNA could also efficiently reprogram T cells in vivo. Mice that were intravenously injected with CD5/LNPs containing luciferase mRNA (CD5/LNP-Luc) were found to express abundant luciferase activity in their splenic T cells, whereas mice injected with isotype control (nontargeting) IgG/LNP-Luc did not (Fig. 2A). Bioluminescence imaging demonstrated spleen targeting only in CD5/LNP-Luc–treated animals (fig. S2A). Liver expression of LNP-delivered mRNA was observed in both CD5/LNP-Luc– and IgG/LNP-Luc–treated animals, as expected mainly due to normal hepatic clearance of LNPs, as reported previously (*22*, *24*). In another experiment, CD5/LNPs were loaded with mRNA encoding Cre recombinase (CD5/LNP-Cre) and injected into Ai6 Cre-reporter mice (Rosa26$^{CAG\text{-}LSL\text{-}ZsGreen}$). We found evidence of genetic recombination (ZsGreen expression) specifically in CD3$^+$ T cells (both CD4$^+$ and CD8$^+$ subsets) from CD5/LNP-Cre–injected animals but little evidence of Cre recombinase

[1]Department of Cell and Developmental Biology, Perelman School of Medicine at the University of Pennsylvania, Philadelphia, PA, USA. [2]Penn Cardiovascular Institute, Perelman School of Medicine at the University of Pennsylvania, Philadelphia, PA, USA. [3]Institute for Regenerative Medicine, Perelman School of Medicine at the University of Pennsylvania, Philadelphia, PA, USA. [4]Department of Medicine, Perelman School of Medicine at the University of Pennsylvania, Philadelphia, PA, USA. [5]Acuitas Therapeutics, Vancouver, British Columbia V6T 1Z3, Canada. [6]Center for Cellular Immunotherapies, Perelman School of Medicine, University of Pennsylvania, Philadelphia, PA, USA. [7]Department of Biomedical Sciences, School of Veterinary Medicine, University of Pennsylvania, Philadelphia, PA, USA.
***Corresponding author. Email: haig@pennmedicine.upenn.edu (H.A.); dreww@pennmedicine.upenn.edu (D.W.); parhizh@pennmedicine.upenn.edu (H.P.); epsteinj@upenn.edu (J.A.E.)**
†These authors contributed equally to this work.
‡Present address: Department of General Thoracic Surgery, Osaka International Cancer Institute, Osaka, Japan.

Corrected 31 October 2022. See full text.



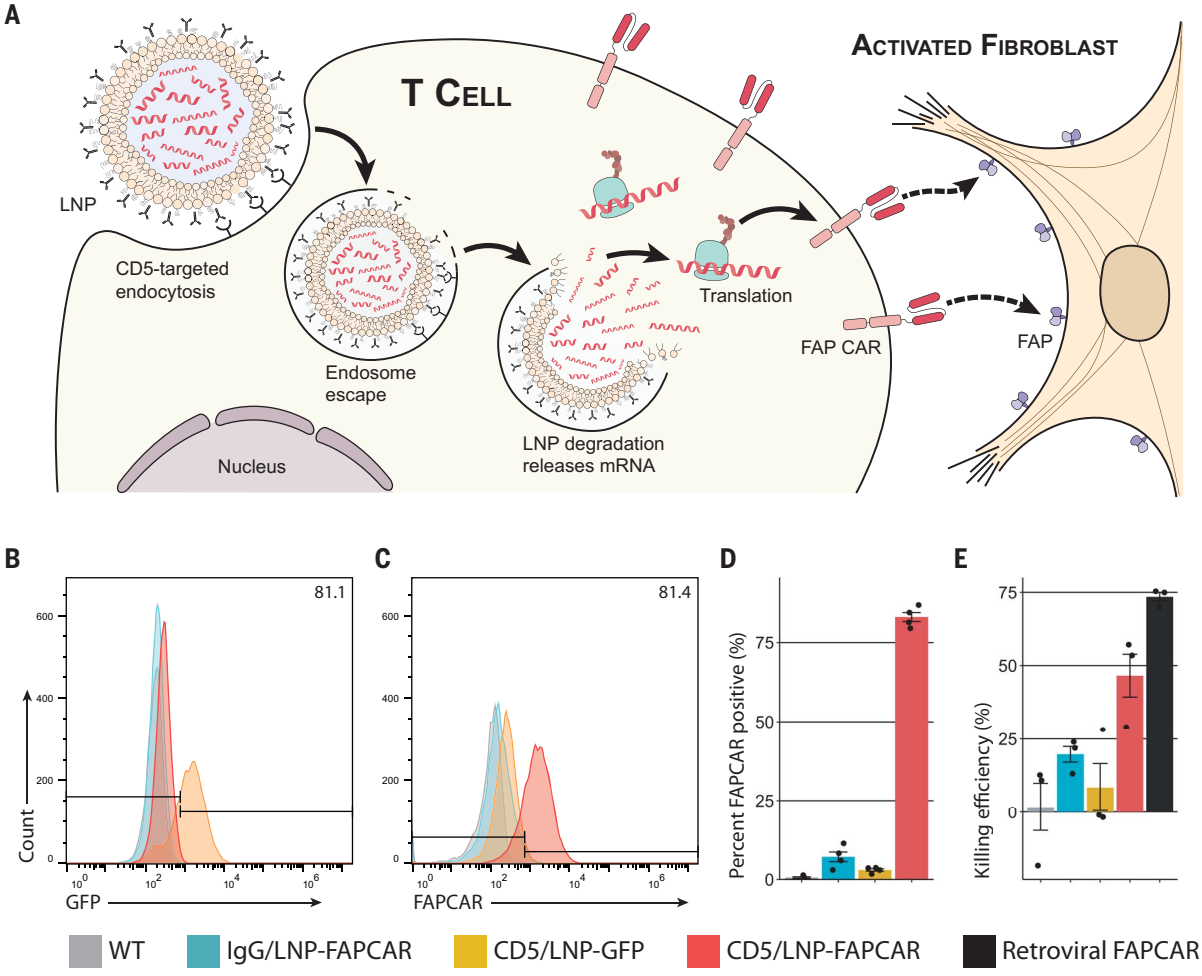


**Fig. 1. CD5-targeted LNPs produce functional, mRNA-based FAPCAR T cells in vitro.** (**A**) Schematic outlining the molecular process to create transient FAPCAR T cells using CD5-targeted LNPs. (**B** and **C**) Representative flow cytometry analysis of GFP (B) and FAPCAR (C) expression in murine T cells 48 hours after incubation with IgG/LNP-FAPCAR, CD5/LNP-GFP, or CD5/LNP-FAPCAR. (**D**) Quantification of murine T cells (percentage) staining positive for FAPCAR from biologically independent replicates ($n$ = 4). (**E**) FAPCAR T cells were mixed with FAP-expressing target HEK293T cells overnight and assayed for killing efficiency in biologically independent replicates ($n$ = 3). Data are shown as mean ± SEM.

activity in $CD3^-$ (non-T) cells (mainly representing B cells, dendritic cells, and macrophages) or in IgG/LNP-Cre–injected mice (Fig. 2B). We next investigated whether targeted LNPs could deliver FAPCAR mRNA (CD5/LNP-FAPCAR) to T cells in an established murine hypertensive model of cardiac injury and fibrosis produced by constant infusion of angiotensin II/phenylephrine (AngII/PE) through implanted 28-day osmotic mini-pumps (*9*, *28*). Mice were injured for 1 week to allow fibrosis to be established before injecting CD5/LNP-FAPCAR (*9*). Forty-eight hours after LNP injection, we found a consistent population of $FAPCAR^+$ T cells (17.5-24.7%) exclusively in mice that received CD5/LNP-FAPCAR (Fig. 2, C and D, and fig. S2B). By contrast, nontargeted (IgG/LNP-FAPCAR) and targeted LNPs containing GFP (CD5/LNP-GFP) did not produce FAPCAR T cells (Fig. 2, C and D, and fig. S2B). We observed FAPCAR expression in each major T cell subset with a slight enrichment in $CD4^+$ T cells above their prevalence in the spleen (of all FAPCAR $T^+$ cells, 87% were $CD4^+$ and 9 to 10% $CD8^+$, with most of both classes portraying a naïve phenotype; 25 to 37% of regulatory T cells were $FAPCAR^+$; fig. S2C and table S1). A mixture of $CAR^+$ T cell subtypes has been shown to benefit CAR effectiveness (*29*). We did not observe significant FAPCAR expression in splenic B cells or natural killer cells (fig. S2C). No FAPCAR expression was found in splenic T cells 1 week after injection, demonstrating the transient nature of FAPCAR expression in this model (table S1).

CAR T cell therapy has previously been associated with a process called trogocytosis, in which lymphocytes extract surface molecules through the immunological synapse from antigen-presenting cells (*30*–*32*) (Fig. 3A). We sought to determine whether FAPCAR T cells produced either in vivo with CD5/LNP-FAPCAR mRNA or adoptively transferred ex vivo virally engineered CAR T cells exhibit evidence of trogocytosis as further support that functional FAPCAR T cells are produced in situ. First, we mixed retrovirus-engineered FAPCAR T cells with human embryonic kidney (HEK) 293T cells overexpressing red fluorescence protein (RFP)–tagged FAP in vitro and observed trogocytosis with live-imaging confocal microscopy (Fig. 3B and movie S1). Immunofluorescence analysis of spleens from AngII/PE–injured animals treated with adoptively transferred, virally transduced GFP-tagged FAPCAR T cells revealed extensive FAP staining in the white pulp regions of the spleen, which was not seen in injured animals treated with control T cells or in uninjured animals (Fig. 3C and fig. S3).

Corrected 31 October 2022. See full text.



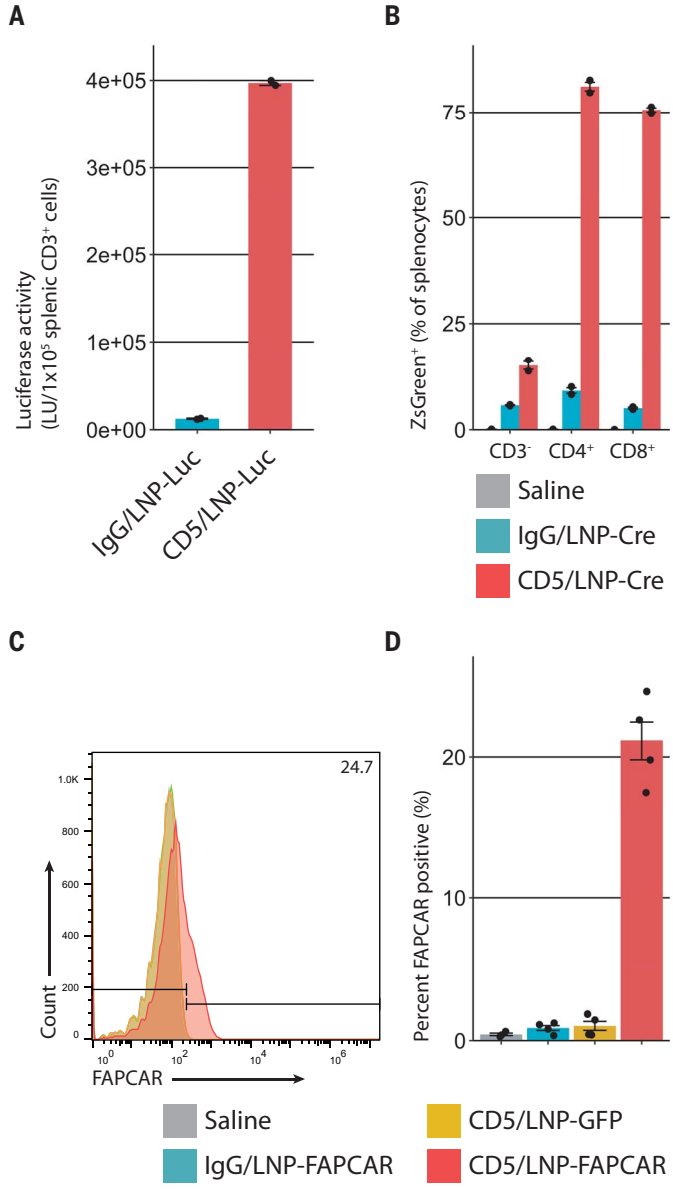


**Fig. 2. CD5-targeted LNPs produce mRNA-based FAPCAR T cells in vivo.** (**A**) Luciferase activity in $CD3^+$ splenocytes 24 hours after intravenous injection of 8 μg of control IgG/LNP-Luc or CD5/LNP-Luc. Bar graphs represent two biologically independent replicates. (**B**) Ai6 mice ($Rosa26^{CAG\text{-}LSL\text{-}ZsGreen}$) were injected with saline or 30 μg of either IgG/LNP-Cre or CD5/LNP-Cre. After 24 hours, ZsGreen expression was observed in 81.1% of $CD4^+$ splenocytes and in 75.6% of $CD8^+$ splenocytes, but in only 15.0% of $CD3^-$ splenocytes. Bar graphs represent two biologically independent replicates. (**C**) T cells were isolated from the spleens of AngII/PE–injured mice 48 hours after injection of 10 μg of LNPs. Representative flow cytometry analysis shows FAPCAR expression in animals injected with CD5/LNP-FAPCAR but not in control saline, IgG/LNP-FAPCAR, or CD5/LNP-GFP animals. (**D**) Quantification of murine T cells staining positive for FAPCAR in (C). $n = 4$ biologically independent mice in two separate cohorts. Data are shown as mean ± SEM.

The $FAP^+$ cells in the spleens of injured and treated animals co-stained for GFP, which indicates that they were transduced cells (Fig. 3D). Furthermore, the FAP staining appeared as cytoplasmic punctae consistent with trogocytosis (Fig. 3D). We observed some rare $FAP^+/GFP^-$ cells in the spleens of injured, treated animals that were not observed in the controls (Fig. 3D, arrow). $CD3^+$ lymphocytes containing $FAP^+$ punctae were also seen in the spleens of injured animals treated with CD5/LNP-FAPCAR therapy but not in those treated with IgG/LNP-FAPCAR control (Fig. 3E). We are not aware of prior reports of CAR T cells exhibiting trogocytosis in the spleen after therapy, perhaps because prior studies have focused on CAR T cells directed against lymphocytic markers that would be difficult to distinguish from endogenous expression in the spleen. These findings are consistent with functional anti-FAP CAR T cells being produced in vivo after CD5/LNP-FAPCAR treatment.

We next assessed whether CD5/LNP-FAPCAR treatment was able to improve cardiac function in injured mice, as was observed previously (*9*). To test this, we induced cardiac injury in mice with AngII/PE delivered through 28-day osmotic mini-pumps. After 1 week, when fibrosis is apparent (*9*), 10 μg of LNPs were injected intravenously. Two weeks after injection, cardiac function was analyzed by echocardiography (Fig. 4A and fig. S4, A and B). We observed marked functional improvements in injured mice treated with in vivo–produced, transient FAPCAR T cells, consistent with our previous studies using adoptively transferred viral FAPCAR T cells (movies S2 to S5). AngII/PE–injured mice treated with CD5/LNP-FAPCAR exhibited normalized left ventricular (LV) end diastolic and end systolic volumes (Fig. 4, B and C). Also consistent with our previous study (*9*), body weight–normalized LV mass (estimated in M-mode) did not show statistically significant differences after CD5/LNP-FAPCAR injection, although a trend in improvement compared with control injured mice was noted (Fig. 4D). LV diastolic function ($E/e'$) returned to uninjured levels (Fig. 4E). LV systolic function was also noticeably improved, as measured by ejection fraction (Fig. 4F) and global longitudinal strain (Fig. 4, G and H). Injection of nontargeting IgG/LNP-FAPCAR did not alter LV function (fig. S4C). In CD5/LNP-FAPCAR–injected animals, but not in controls, we observed an accumulation of $CD3^+$ T cells within regions occupied by $FAP^+$ fibroblasts (fig. S4D) (*9*). Furthermore, many of these $CD3^+$ T cells were $FAPCAR^+$ (80 of 137, or 58% of $CD3^+$ T cells observed in 25 highly magnified fields of view in five histologic sections), indicating that they had been transduced with FAPCAR mRNA, whereas $CD3^+$ T cells from control animals did not co-stain for the FAPCAR (fig. S4E). Consistent with our previous results (*9*), we observed a statistically significant improvement of the heart weight to body weight ratio (a measure of cardiac hypertrophy) in treated animals (fig. S5A).

Histologic analysis, as assessed by staining with picrosirius red, highlighted a significant improvement in the overall burden of extracellular matrix between injured mice treated with CD5/LNP-FAPCAR and those treated with saline or IgG/LNP-FAPCAR controls (Fig. 4, I and J, and fig. S5, B and C). Furthermore, a subset of treated animals (five of 12) was indistinguishable from uninjured controls, apart from the persistent perivascular fibrosis that results from activated fibroblasts that do not express FAP (*9*) (fig. S5D, arrows). Previous studies in which activated fibroblasts were eliminated by genetic ablation or treatment with virally transduced CAR T cells have also shown persistence of perivascular fibrosis (*9*, *28*). Thus, CD5/LNP-FAPCAR treatment results in improved function and decreased interstitial fibrosis. We did not observe any gross histological changes in noncardiac organs or weight loss after CD5/LNP-FAPCAR injection (fig. S6, A and B).

These experimental results provide a proof of concept that modified mRNA encapsulated in targeted LNPs can be delivered intravenously to produce functional engineered T cells in vivo. The marked success and safety

Corrected 31 October 2022. See full text.



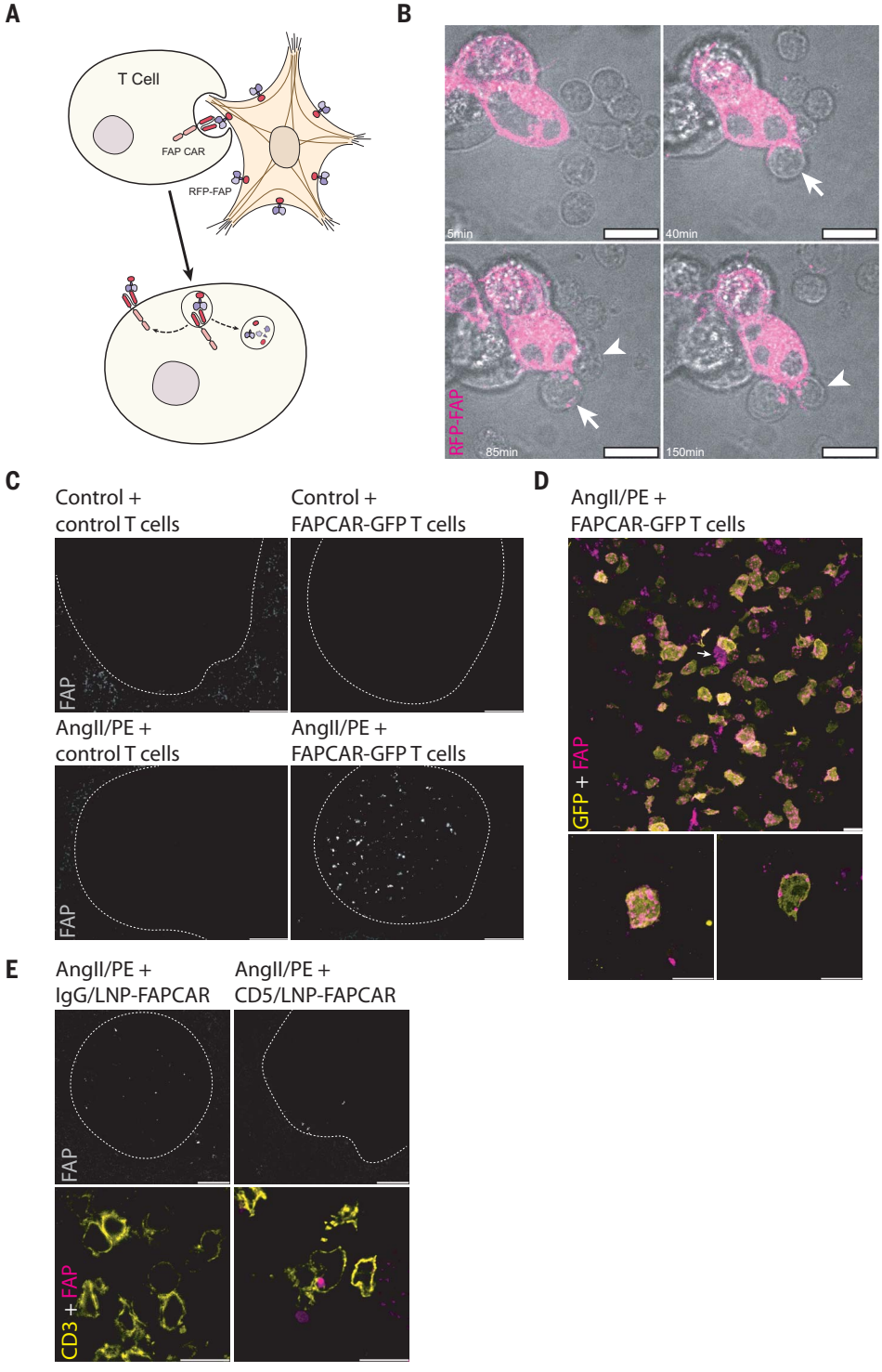


**Fig. 3. FAPCAR T cells trogocytose FAP from activated cardiac fibroblasts and return FAP to the spleen only in AngII/PE–injured, FAPCAR T cell–treated animals.** (**A**) Schematic representation of FAPCAR-expressing T cells trogocytosing FAP from activated fibroblasts. (**B**) Confocal time-lapse micrographs of two FAPCAR T cells first forming an immunological synapse at 40 min (arrow) and 85 min (arrowhead) and then trogocytosing RFP-FAP (magenta) from HEK293T cells [punctae can be seen at 85 min (arrow) and at 150 min (arrowhead) within FAPCAR T cells]. Scale bars, 10 μm. (**C**) Wide-field images of FAP-stained spleens (white pulp regions highlighted by the dashed line) of an uninjured animal 24 hours after adoptive transfer of $10^7$ MigR1-control T cells, an uninjured animal 24 hours after adoptive transfer of $10^7$ FAPCAR-GFP T cells, an AngII/PE–injured (7 days) animal 48 hours after adoptive transfer of $10^7$ MigR1-control T cells, and an AngII/PE–injured (7 days) animal 48 hours after adoptive transfer of $10^7$ FAPCAR-GFP T cells. Scale bars, 100 μm. (**D**) Confocal micrograph of FAP (magenta) and FAPCAR-GFP (yellow) in a white pulp region of the spleen of an AngII/PE–injured (7 days) animal 48 hours after adoptive transfer of $10^7$ FAPCAR-GFP T cells. Shown are a maximum *Z* projection (lower left subpanel) and a single *Z* slice (lower right subpanel) of a representative $FAP^+/FAPCAR^+$ T cell. Scale bars, 10 μm. (**E**) Confocal micrographs of a white pulp region (dashed outline) of FAP-stained spleens from AngII/PE–injured (7 days) animals injected with 10 μg of IgG/LNP-FAPCAR or CD5/LNP-FAPCAR for 48 hours. FAP (gray and magenta) and CD3 (yellow) overlap specifically in the CD5/LNP-FAPCAR–treated condition. Scale bars, 100 μm (top row, grayscale) or 10 μm (bottom row, merged pseudocolored).

of modified mRNA/LNP severe acute respiratory syndrome coronavirus 2 (SARS-CoV-2) vaccines has stimulated broad efforts to extend this therapeutic platform to address numerous pathologies. By targeting LNPs to specific cell types, as we demonstrate here for lymphocytes, modified mRNA therapeutics are likely to have far-reaching applications. The generation of engineered T cells in vivo using mRNA is attractive for certain disorders because the transient nature of the produced CAR T cells is likely to limit toxicities, including risks incurred by lymphodepletion before injection, and allow for precise dosing. Unlike patients with cancer, those suffering from fibrotic disorders may not require a complete elimination of pathologic cells (activated fibroblasts) but may symptomatically benefit from an overall reduction in burden of disease. Furthermore, targeted LNP/mRNA technology affords the advantageous ability to titrate dosing and to re-dose as needed. Future studies will be needed to optimize the dosing strategy, LNP composition, and targeting approaches to

Corrected 31 October 2022. See full text.



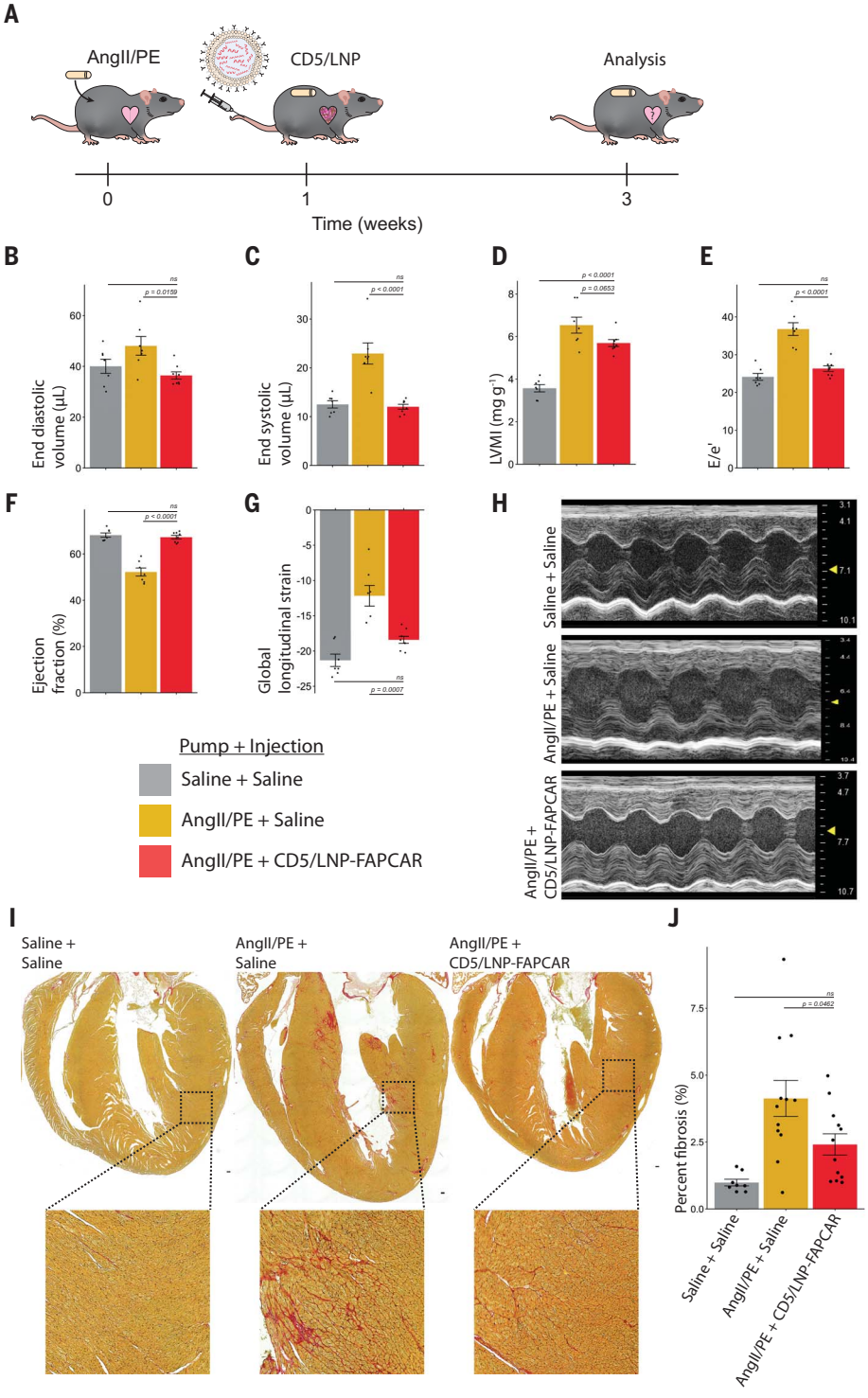


**Fig. 4. In vivo generation of transient FAPCAR T cells improves cardiac function after injury.** Wild-type adult C57BL/6 mice were continuously dosed with saline or AngII/PE through an implanted 28-day osmotic minipump. After 1 week of cardiac pressure–overload injury, CD5-targeted LNPs were injected. Mice were analyzed after an additional 2 weeks. (**A**) Schematic representation of the experimental timeline. Echocardiograph measurements show improvements in LV volumes and diastolic and systolic function after a single injection of 10 μg of CD5/LNP-FAPCAR. (**B** and **C**) Measurements of end diastolic (B) and end systolic (C) volumes (in microliters). (**D**) M-mode estimate of weight-normalized LV mass (in milligrams per gram). (**E** to **G**) Diastolic function (*E*/*e*'), an estimate of LV filling pressure (E); ejection fraction [percent (F)]; and global longitudinal strain (G). (**H**) Representative M-mode echocardiography images. Echocardiograph data represent $n = 7$, $n = 7$, and $n = 8$ biologically independent mice per condition spread over three cohorts. (**I**) Picrosirius red staining highlights collagen (pink) in coronal cardiac sections of mock uninjured animals (3 weeks after saline pump implant + saline injection at week 1), injured control animals (AngII/PE + saline), and treated animals (AngII/PE + CD5/LNP-FAPCAR). Inset shows magnification of the LV myocardium. Scale bar, 100 μm. (**J**) Quantification of fibrosis (percentage) of the ventricles seen in (I). Histology data represent $n = 8$, $n = 11$, and $n = 12$ biologically independent mice per condition spread over five cohorts. Data are shown as mean ± SEM. *P* values shown are from Tukey's post hoc test after one-way ANOVA ($P < 0.05$).

further enhance therapeutic effects and limit potential toxicities. Nevertheless, the possibility of an "off-the-shelf" universal therapeutic capable of engineering specific immune functions provides promise for a scalable and affordable avenue to address the enormous medical burden of heart failure and other fibrotic disorders.

## REFERENCES AND NOTES


1. H. Khalil *et al.*, *J. Clin. Invest.* **127**, 3770–3783 (2017).
2. S. Schafer *et al.*, *Nature* **552**, 110–115 (2017).
3. T. Moore-Morris *et al.*, *J. Clin. Invest.* **124**, 2921–2934 (2014).
4. T. Yokota *et al.*, *Cell* **182**, 545–562.e23 (2020).
5. J. G. Rurik, H. Aghajanian, J. A. Epstein, *Circ. Res.* **128**, 1766–1779 (2021).
6. A. A. Widjaja *et al.*, *Front. Mol. Biosci.* **8**, 740650 (2021).
7. N. C. Henderson, F. Rieder, T. A. Wynn, *Nature* **587**, 555–566 (2020).
8. A. González, E. B. Schelbert, J. Díez, J. Butler, *J. Am. Coll. Cardiol.* **71**, 1696–1706 (2018).
9. H. Aghajanian *et al.*, *Nature* **573**, 430–433 (2019).
10. M. Kalos *et al.*, *Sci. Transl. Med.* **3**, 95ra73 (2011).
11. D. Weissman, *Expert Rev. Vaccines* **14**, 265–281 (2015).
12. K. Karikó, M. Buckstein, H. Ni, D. Weissman, *Immunity* **23**, 165–175 (2005).
13. K. Karikó *et al.*, *Mol. Ther.* **16**, 1833–1840 (2008).
14. O. Andries *et al.*, *J. Control. Release* **217**, 337–344 (2015).

Corrected 31 October 2022. See full text.



15. Y. Zhao *et al*., *Cancer Res.* **70**, 9053–9061 (2010).
16. N. Pardi, M. J. Hogan, F. W. Porter, D. Weissman, *Nat. Rev. Drug Discov.* **17**, 261–279 (2018).
17. F. Rizvi *et al*., *Nat. Commun.* **12**, 613 (2021).
18. C. Krienke *et al*., *Science* **371**, 145–153 (2021).
19. D. Szőke *et al*., *Nat. Commun.* **12**, 3460 (2021).
20. J. D. Gillmore *et al*., *N. Engl. J. Med.* **385**, 493–502 (2021).
21. N. Pardi *et al*., *J. Control. Release* **217**, 345–351 (2015).
22. A. Akinc *et al*., *Mol. Ther.* **18**, 1357–1364 (2010).
23. H. Parhiz *et al*., *J. Control. Release* **291**, 106–115 (2018).
24. I. Tombácz *et al*., *Mol. Ther.* **29**, 3293–3304 (2021).
25. L. C. S. Wang *et al*., *Cancer Immunol. Res.* **2**, 154–166 (2014).
26. L. Boumsell *et al*., *J. Exp. Med.* **152**, 229–234 (1980).
27. G. Soldevila, C. Raman, F. Lozano, *Curr. Opin. Immunol.* **23**, 310–318 (2011).
28. H. Kaur *et al*., *Circ. Res.* **118**, 1906–1917 (2016).
29. D. Sommermeyer *et al*., *Leukemia* **30**, 492–500 (2016).
30. M. Hamieh *et al*., *Nature* **568**, 112–116 (2019).
31. E. Joly, D. Hudrisier, *Nat. Immunol.* **4**, 815 (2003).
32. N. Martínez-Martín *et al*., *Immunity* **35**, 208–222 (2011).

## ACKNOWLEDGMENTS

We thank A. Kiseleva for technical support and essential pandemic comradery, C. Smith for manuscript comments, N. Olimpo for troubleshooting advice, and the Pathology Core Laboratory at the Children's Hospital of Philadelphia Research Institute for providing picrosirius red staining services. **Funding:** This research was supported by the National Institutes of Health (NIH grants HL134839 and AI124429 to D.W. and grant NIH R35 HL140018 to J.A.E.), the Penn Center for AIDS Research (CFAR), an NIH-funded program (grant P30 AI 045008 to H.P.), the Cotswold Foundation (J.A.E.), and a W.W. Smith endowed chair to J.A.E.

**Author contributions:** J.G.R., H.A., D.W., H.P., and J.A.E. conceived of the project and designed experiments. J.G.R., I.T., A.Y., P.O.M.F., S.V.S., L.L., T.K., O.Y.S., T.E.P., H.A., and H.P. performed experiments. Y.K.T. and B.L.M. designed and produced the LNPs. J.G.R., H.A., and J.A.E. interpreted the data. J.G.R. and J.A.E. wrote the manuscript. J.G.R., I.T., A.Y., S.M.A., E.P., C.H.J., H.A., D.W., H.P., and J.A.E. edited the manuscript. J.A.E. supervised all aspects of the research. **Competing interests:** S.M.A., E.P., C.H.J., H.A., D.W., H.P., and J.A.E. are scientific founders and hold equity in Capstan Therapeutics. Y.K.T. and B.L.M. are employees and hold equity in Acuitas Therapeutics. S.M.A. is on the scientific advisory boards of Verismo and Bioardis. C.H.J. is a scientific founder and has equity in Tmunity Therapeutics and DeCART Therapeutics, reports grants from Tmunity Therapeutics, and is on the scientific advisory boards of BluesphereBio, Cabaletta, Carisma, Cellares, Celldex, ImmuneSensor, Poseida, Verismo, Viracta Therapeutics, WIRB Copernicus Group, and Ziopharm Oncology. D.W. receives research support from BioNTech. S.M.A., E.P., and C.H.J. are inventors (University of Pennsylvania, Wistar Institute) on a patent for a FAP CAR (US Utility Patent 9,365,641 issued 14 June 2016, WIPO Patent Application PCT/US2013/062717). S.M.A., E.P., H.A., and J.A.E. are inventors (University of Pennsylvania) on a patent for the use of CAR T therapy in heart disease (US Provisional Patent Application 62/563,323 filed 26 September 2017, WIPO Patent Application PCT/US2018/052605). J.G.R., I.T., H.A., D.W., H.P., and J.A.E. are inventors (University of Pennsylvania) on a patent for the use of CD5/LNP-FAPCAR as an antifibrotic therapy (US Provisional Patent Application 63/090,998 filed 13 September 2020, WIPO Patent Application PCT/ US21/54764 filed 13 October 2021). I.T., D.W., and H.P. are inventors (University of Pennsylvania) on a patent for the in vivo targeting of T cells for mRNA therapeutics (US Provisional Patent Application 63/090,985 filed 13 October 2020, WIPO Patent Application PCT/US21/54769 filed 13 October 2021). I.T., D.W., and H.P. are inventors (University of Pennsylvania) on a patent for the in vivo targeting of $CD4^+$ T cells for mRNA therapeutics (US Provisional Patent Application 63/091,010 filed 13 October 2020, WIPO Patent Application PCT/US21/54775). In accordance with the University of Pennsylvania policies and procedures and our ethical obligations as researchers, D.W. and H.P. are named on additional patents that describe the use of nucleoside-modified mRNA and targeted LNPs as platforms to deliver therapeutic proteins and vaccines. C.H.J. is named on additional patents that describe the creation and therapeutic use of chimeric antigen receptors. These interests have been fully disclosed to the University of Pennsylvania, and approved plans are in place for managing any potential conflicts arising from licensing these patents. **Data and materials availability:** All data are available in the main manuscript or the supplementary materials. Requests for materials should be addressed to H.A., D.W., H.P., or J.A.E.

## SUPPLEMENTARY MATERIALS

science.org/doi/10.1126/science.abm0594
Materials and Methods
Figs. S1 to S6
Movies S1 to S5
Table S1
References (*33*–*36*)
MDAR Reproducibility Checklist

View/request a protocol for this paper from *Bio-protocol*.

23 August 2021; accepted 3 November 2021
10.1126/science.abm0594